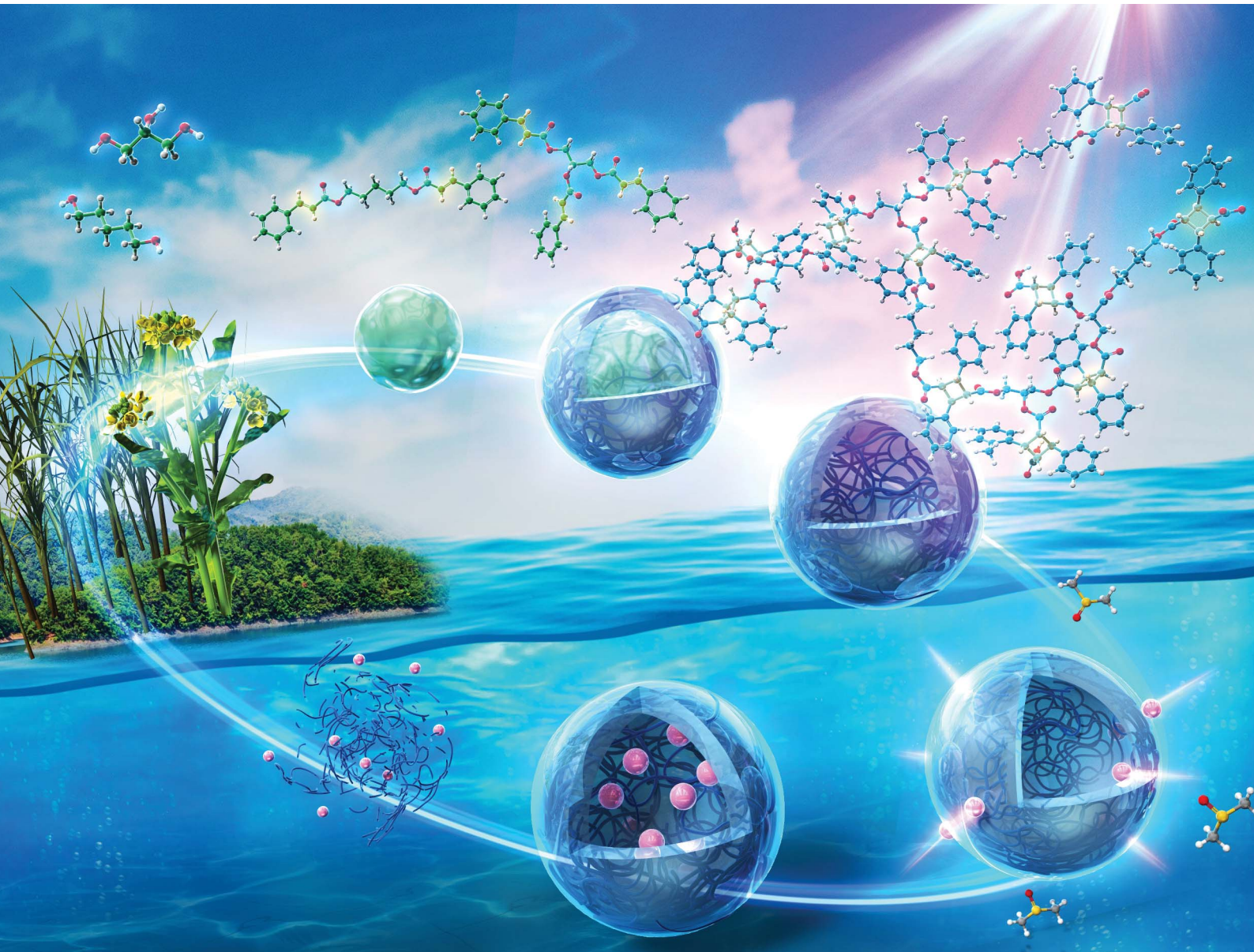


Chemical Science

rsc.li/chemical-science



ISSN 2041-6539

EDGE ARTICLE

Yukiya Kitayama, Atsushi Harada *et al.*
Interfacial photocycloaddition polymerization: a synthetic
approach for structurally functionalized degradable polymer
particles from naturally derived monomers



Cite this: *Chem. Sci.*, 2026, **17**, 2067

All publication charges for this article have been paid for by the Royal Society of Chemistry

Interfacial photocycloaddition polymerization: a synthetic approach for structurally functionalized degradable polymer particles from naturally derived monomers

Yukiya Kitayama, * Misato Yamashita and Atsushi Harada *

Industrially relevant polymer capsules—structurally functionalized particulate materials that have shown promise for application in cosmetics, fragrances, and agrochemicals—typically comprise non-degradable synthetic polymers that cause marine microplastic pollution, which is a global environmental issue. This paper describes the synthesis of structurally functionalized degradable polymer particles by photolysis and hydrolysis without any initiators or catalysts *via* interfacial photocycloaddition polymerization of natural product-derived photoreactive monomers in aqueous heterogeneous systems. The resultant polymeric particles stably encapsulate dyes and fragrance molecules and decompose into naturally occurring raw materials. The reaction wavelengths for interfacial photocycloaddition polymerization (for capsule synthesis) and retro-photocycloaddition (for photodegradation) can be regulated using photoreactive monomers with appropriate substituents. Moreover, scaled-up synthesis of the polymer capsules is possible using high-power light-emitting diode light. This technology is expected to expedite the design of an innovative synthesis method for resource-recycling polymer capsules that can contribute toward the realization of a sustainable society.

Received 15th October 2025
Accepted 1st November 2025

DOI: 10.1039/d5sc07979a
rsc.li/chemical-science

Introduction

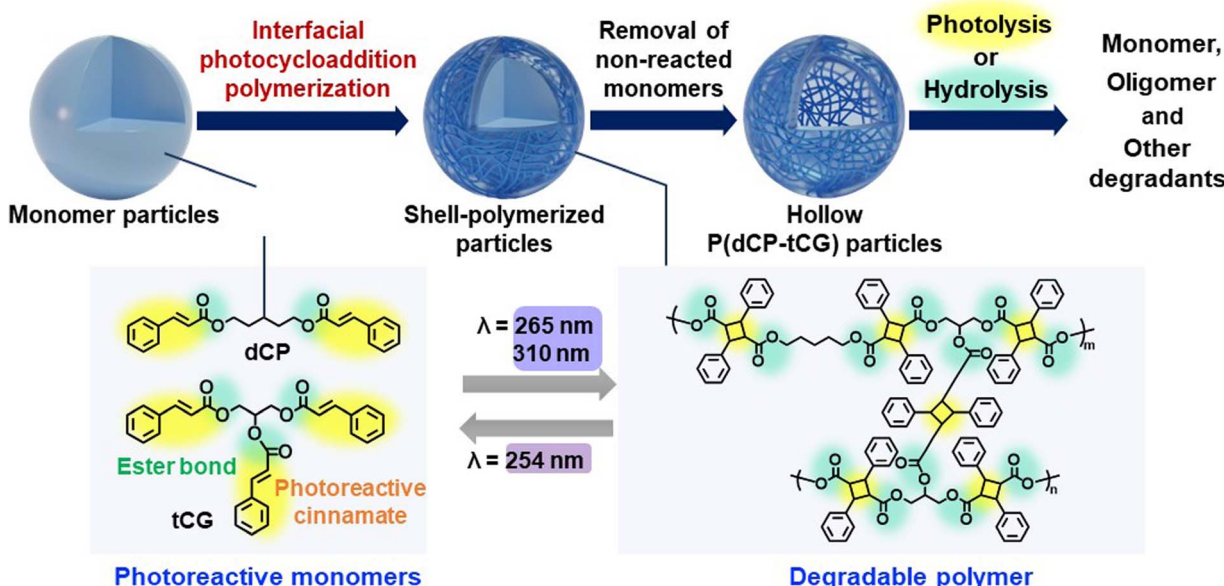
Polymer capsules,^{1–3} representative structurally functionalized polymer particles containing various functional molecules, are used as fragrance materials,^{4,5} sunscreen agents,⁶ and agrochemicals.⁷ Additionally, polymer capsules with internal voids and hollow polymer particles⁸ are widely used in industrial applications and cosmetics owing to their unique light-scattering properties.^{9–11} Currently, most polymer capsules used in industry comprise non-degradable petroleum-based plastics. Owing to their small size, polymer capsules are easily dispersed in the environment, causing marine microplastic pollution, an emerging issue requiring resolution worldwide through the development of innovative technologies.^{12–14} Besides adsorbing harmful chemicals, microplastics spilled into the ocean¹⁵ enter fish and other marine organisms *via* aspiration,¹⁶ potentially affecting marine ecosystems and human health.^{17,18} To date, various approaches have been proposed for synthesizing polymer capsules, including templating methods utilizing layer-by-layer deposition,^{19,20} seeded polymerization,²¹ surface-initiated polymerization²² with removable inorganic templates, suspension polymerization

utilizing the self-assembly of phase-separated polymers,²³ interfacial radical polymerization,^{24–26} interfacial polyaddition,²⁷ and interfacial polycondensation²⁸ with droplet templates. Recent studies have reported the interfacial photocrosslinking of polymer particles with photoreactive side chains for the synthesis of polymer capsules.^{29,30} Using this approach, hollow polymer particles with a dense polymer shell can be manufactured directly from spherical polymer particles without templates in a simple process involving photoirradiation and washing. These polymer particles can be used to fabricate capsules for encapsulating a variety of molecules, including drugs, dyes, polysaccharides, and oligonucleotides.³¹ Furthermore, multifunctional polymer capsules can be easily prepared by introducing properties such as pH responsiveness,³¹ reduction responsiveness,³² and photo-induced decrosslinking³³ into the photoreactive polymer particles. Nevertheless, the capsules developed in this study were constructed from vinyl polymers, which are generally non-biodegradable under natural environmental conditions.

In this study, interfacial photocycloaddition polymerization of multifunctional photoreactive monomers was proposed as a novel approach to fabricate degradable hollow and capsule polymer particles by photolysis and hydrolysis (Scheme 1). In this polymerization, the elementary reaction is a $[2\pi + 2\pi]$ photodimerization reaction between photoreactive cinnamate groups without initiators or catalysts. The reaction proceeds in

Department of Applied Chemistry, Graduate School of Engineering, Osaka Metropolitan University, 1-1, Gakuen-cho, Naka-ku, Sakai, Osaka 599-8531, Japan.
E-mail: kitayama@omu.ac.jp; atsushi_harada@omu.ac.jp





Scheme 1 Interfacial photocycloaddition polymerization for synthesizing degradable hollow polymer particles capable of hydrolytic and photolytic degradation.

water, which is an environment-friendly medium and does not inhibit the photodimerization reaction. The hollow polymeric particles were synthesized from natural products and were designed to decompose into naturally occurring raw materials (Scheme 1). This study presents the first example of a method for preparing hollow polymer particles based on interfacial photoreactions of monomer particles, using environmentally benign water as the solvent, without the need for any initiators or catalysts. Through the development of this technology, this study aims to establish an innovative approach to synthesize degradable polymer capsules that can contribute to the establishment of a sustainable society.

Results and discussion

Interfacial photocycloaddition polymerization

To develop the interfacial photocycloaddition polymerization, dicinnamoyl pentanediol (dCP) and tricinnamoyl glycerin (tCG) were synthesized as a bifunctional and trifunctional photoreactive monomer, respectively, from 1,5-pentanediol and glycerin *via* a coupling reaction with cinnamoyl chloride, a derivative of the naturally occurring cinnamic acid found in various plants. 1,5-Pentanediol is produced from glucose in *Escherichia coli* *via* a lysine-derived artificial pathway.^{34,35} Glycerin combines with fatty acids and is stored in human and animal bodies. The syntheses of dCP and tCG were confirmed by ¹H and ¹³C NMR analyses (Fig. S1–S4). The maximum absorption wavelengths of dCP and tCG (~280 nm) can be attributed to the cinnamate groups (Fig. S5 and S6). Moreover, both monomers were solids at 25 °C; the melting points of dCP and tCG were determined to be 43 and 74 °C, respectively.

In this study, micrometer-sized solid monomer particles were prepared by solvent evaporation from chloroform droplets

containing dCP and tCG (in a 1:1 molar ratio), fabricated by homogenization in a poly(vinyl alcohol) aqueous solution (total monomer weight: 2 mg; dispersion volume: 3 mL). The number-average size (diameter) of the solid monomer particles was ~4.4 μm (with a coefficient of variation (CV) of 20%) (Fig. 1b and c). Monomer particles could be prepared using ethyl acetate as the organic solvent instead of chloroform (Fig. S7), where ethyl acetate is a more safe natural compound found in various fruits such as pineapples and strawberries.^{36,37} Furthermore, monomer particles could be prepared by using a high-solid-content monomer/chloroform droplet dispersion in a poly(vinyl alcohol) aqueous solution (~16.7 vol%, which is the ratio of monomer/chloroform volume to total volume) (Fig. S8). The solid content of the monomer particles in the aqueous phase successfully increased to approximately 10 wt%, which is the ratio of the weight of the monomer to total monomer dispersion (Fig. S9). After preparation of the solid monomer particles, interfacial photocycloaddition polymerization was conducted by photoirradiating the photoreactive monomer particles containing dCP and tCG for 16 h with light-emitting diode (LED) light ($\lambda = 265$ nm at the maximum absorption wavelength (LED_{265}); 4 mW cm⁻²; 78.5 mm²) (Fig. 1a). A time-conversion plot was prepared using the absorbance data of the unreacted cinnamates (Fig. 1f and g). With increasing photoirradiation time, the absorbance at $\lambda = 280$ nm (derived from cinnamates) decreases, indicating the progress of the $[2\pi + 2\pi]$ photocycloaddition reaction. However, the conversion value was saturated at approximately 70%, suggesting that the photocycloaddition polymerization only proceeded partially. Upon photoirradiation, step-growth polymerization based on the $[2\pi + 2\pi]$ photodimerization reaction between cinnamate groups of the solid monomer particles proceeds preferentially from the interfacial region. However, some cinnamate groups lack



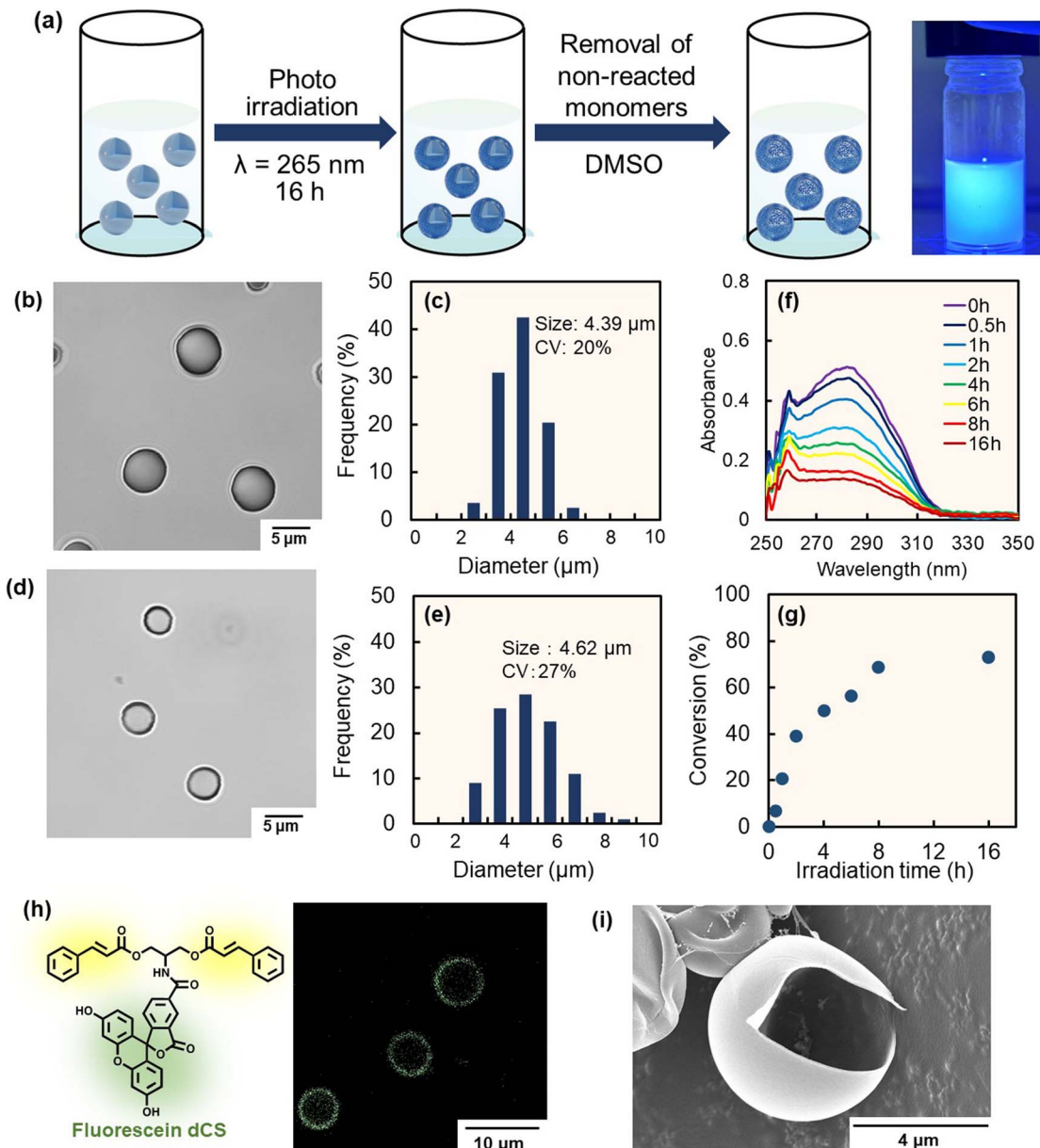


Fig. 1 Schematic of interfacial photocycloaddition polymerization for the synthesis of degradable hollow polymer particles *via* photolysis and hydrolysis (a). Optical microscopy images (b and d) and particle size distributions (c and e) of the monomer particles used as starting materials (b and c) and hollow particles synthesized through interfacial photocycloaddition polymerization (d and e). UV-vis spectra (f) and conversion (%) (g) derived from non-reacted cinnamates after interfacial photocycloaddition polymerization for various photoirradiation times. CLSM images of hollow polymer particles copolymerized with fluorescein dCS (h). A scanning electron microscopy image of a synthesized hollow particle (i).

neighboring cinnamoyl groups; although they absorb light, they do not undergo the dimerization reaction. Consequently, these cinnamate groups exert a light-shielding effect. As a result, polymerization occurs predominantly at the interface, while the reaction does not sufficiently progress in the core region. This interfacial selectivity of the photoreaction between cinnamate groups was previously demonstrated in polymer film systems.²⁹

To confirm interfacial photocycloaddition polymerization, the washing process of the photoirradiated particles prepared with 16 h of photoirradiation was directly observed using optical microscopy (Fig. 2a). In these experiments, the

photoirradiated particles were washed with good solvent (dimethyl sulfoxide (DMSO)) to remove unreacted (or non-crosslinked oligomers) from the photoirradiated particles, where DMSO is a compound widely present in nature, formed when dimethyl sulfide produced by marine plankton undergoes photooxidation, and it plays a role in the Earth's sulfur cycle.^{38,39} For the control experiment, particles without photoirradiation were immediately dissolved in good solvents (DMSO) (Fig. 2b and S10, Movie 1). Notably, the photoirradiated particles comprising dCP and tCG underwent swelling upon DMSO addition; a shell layer was observed on the particles, even after

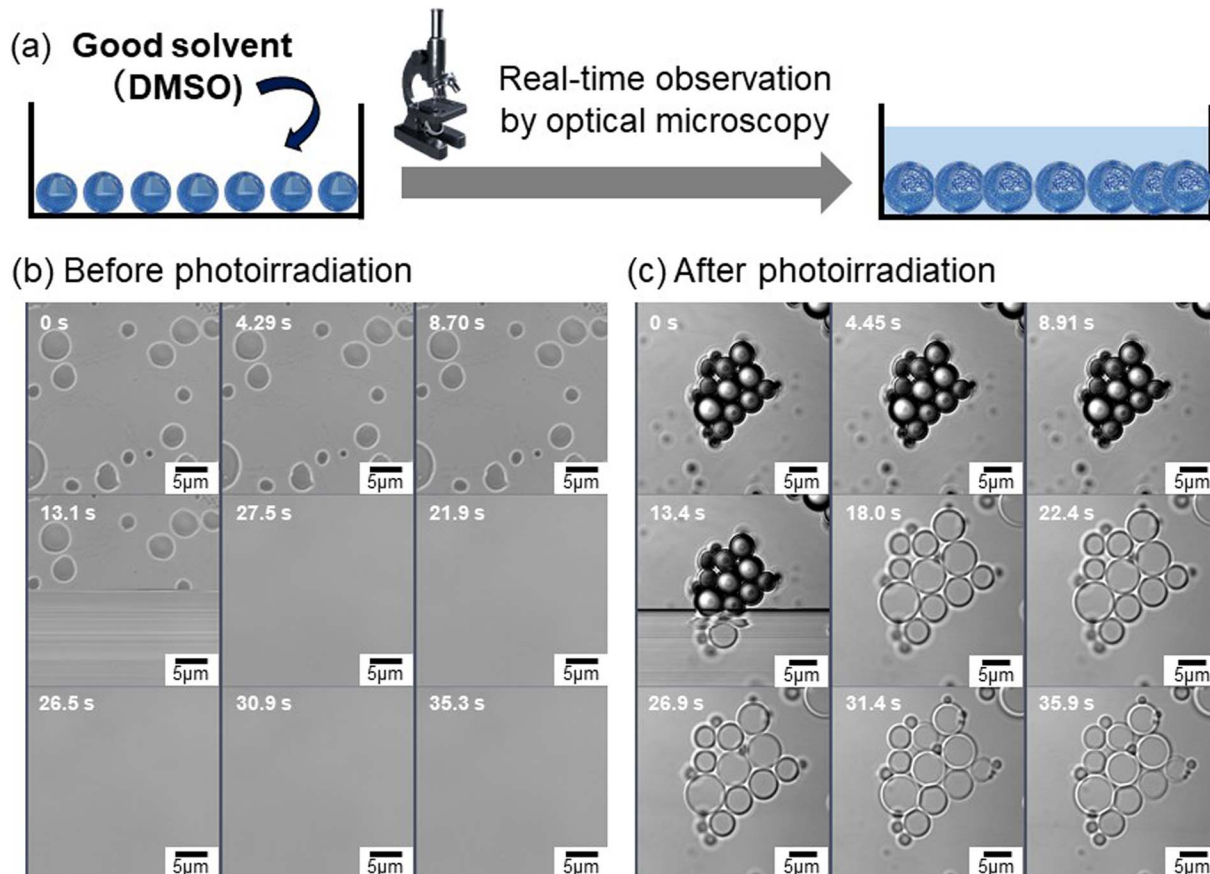


Fig. 2 Schematic of the real-time observation of the washing process of P(dCP-tCG) particles using optical microscopy (a). A series of optical microscopy images used for directly observing the washing process of the P(dCP-tCG) particles without (b) and with (c) LED₂₆₅ photoirradiation.

undergoing an average volume change of ~213% upon swelling in DMSO (Fig. 2c and S10, Movie 2). After washing with DMSO, the polymer particles were further washed with PVA aqueous solution to remove DMSO, resulting in the hollow polymer particles being observed using optical microscopy (Fig. 1d). The number-average particle size of the hollow polymer particles was 4.6 μm (CV: 27%) (Fig. 1e). To observe the internal structure by confocal laser scanning microscopy (CLSM), fluorescein-labeled dicinnamoyl serinol (fluorescein dCS) was synthesized (Fig. S11–S14) and fluorescein-labeled hollow polymer particles were fabricated by the interfacial photocycloaddition polymerization of monomer particles comprising dCP, tCG, and fluorescein dCS. After interfacial photocycloaddition polymerization and subsequent removal of the non-reacted monomers, significant fluorescence was observed in the P(dCP-tCG-fluorescein dCS) shell, whereas negligible fluorescence was observed inside the particles (Fig. 1h). The internal hollow structure and smooth surface of the P(dCP-tCG) particles were directly observed using scanning electron microscopy (SEM; Fig. 1i). The number-average shell thickness of the hollow P(dCP-tCG) particles prepared with 16 h of photoirradiation was evaluated to be approximately 130 nm, based on SEM images of fractured particles, which allowed for direct observation of the shell cross-section. This value also represents the maximum shell thickness attainable under the present experimental conditions, as the conversion of photoreactive groups reached saturation. The gel

content evaluated from the number-average shell thickness and particle size was approximately 16 vol%. Furthermore, to evaluate the gel content, we compared the weight of the hollow particles after washing following photoirradiation with the initial weight of the monomer mixture. Based on this comparison, the gel content was estimated to be approximately 15 wt%. These gel contents and conversion of photoreactive groups suggest that polymerization proceeded near the interface, where a part of the monomers formed a crosslinked network to generate a polymer shell. However, some monomers located farther from the particle interface may have undergone polymerization without forming crosslinked structures and were subsequently removed during the washing process. In contrast to the sufficient photoirradiation times, when the photoirradiation time was reduced to 8 h, the polymer shell underwent insufficient polymerization and cross-linking, which failed to provide adequate mechanical strength and consequently led to a pronounced reduction in the average particle size (Fig. S15). These results indicate that interfacial photocycloaddition polymerization is an effective approach for synthesizing hollow polymer particles directly from photoreactive monomers.

To investigate the monomer composition, interfacial photocycloaddition polymerization was carried out with tCG or dCP. Hollow polymer particles were synthesized by the interfacial photocycloaddition polymerization of tCG (without dCP), as indicated by SEM (Fig. S16). In contrast, the polymer particles

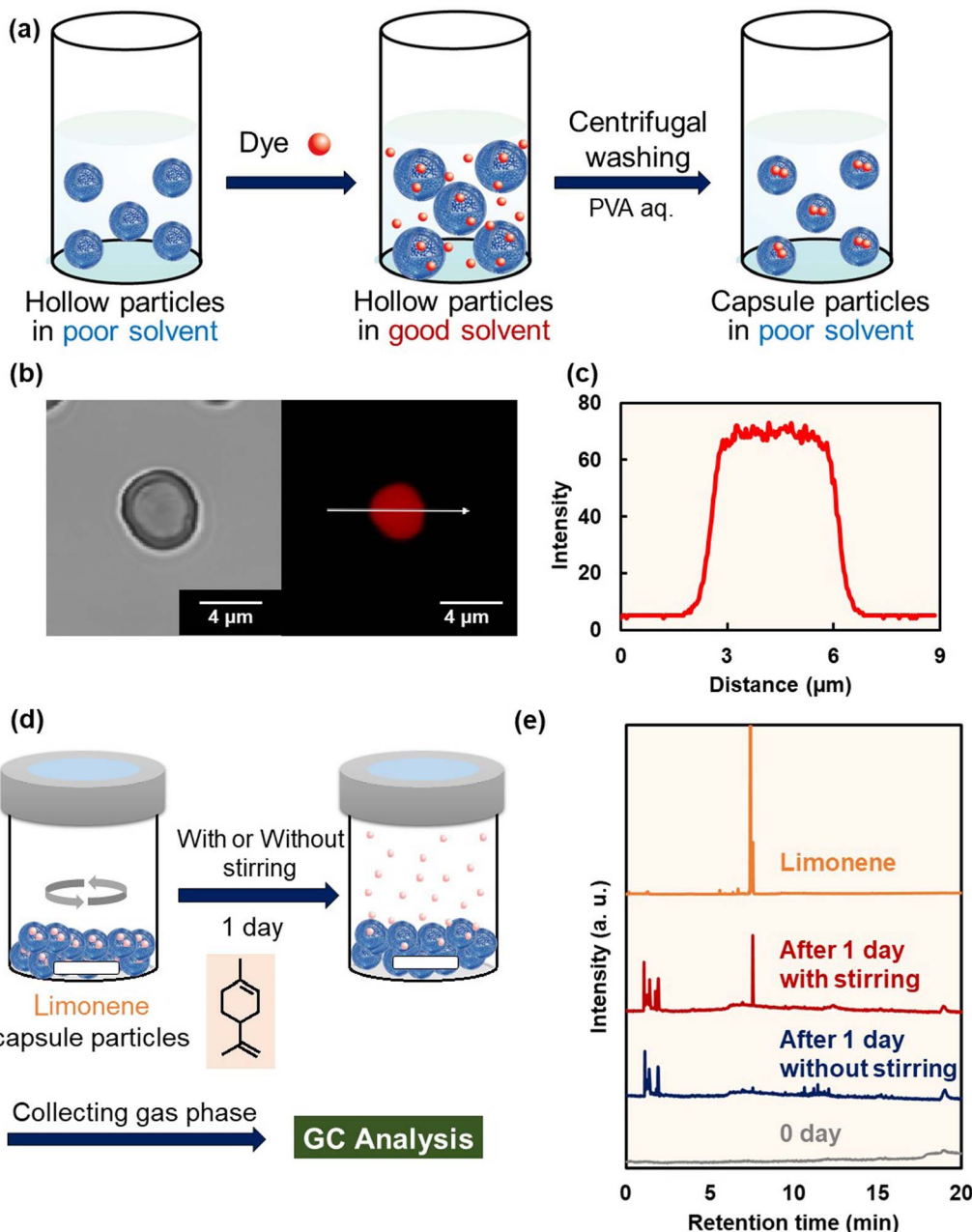


Fig. 3 Schematic of the sulforhodamine B encapsulation process in hollow P(dCP-tCG) particles (a). Bright-field (left) and CLSM (right) images of sulforhodamine B-encapsulated P(dCP-tCG) particles (b). Line profile of the fluorescence intensity of the CLSM image (right) of sulforhodamine B-encapsulated P(dCP-tCG) particles (c). Schematic of gas chromatography (GC) analysis of the gas phase extracted from closed vials containing limonene capsules (d). Chromatographs of GC analysis of limonene and limonene-encapsulated polymer capsules stored for zero and one day with and without stirring (e).

synthesized with dCP (without tCG) dissolved in DMSO (Fig. S17). These results indicate that a trifunctional monomer is required for the synthesis of the target hollow polymer particles. From the viewpoint of degradability, it is desirable to have a low cross-linking density; thus, the copolymer of dCP and tCG is mainly used in the following study. To investigate the effect of the LED wavelength on the proposed synthesis, interfacial photocycloaddition polymerization of dCP and tCG was conducted at LED wavelengths of 310 nm (LED₃₁₀) and 365 nm (LED₃₆₅), in addition to LED₂₆₅. Interfacial photocycloaddition polymerization with

LED₃₁₀ led to the formation of hollow P(dCP-tCG) particles in which the crosslinked polymer shell remained intact in DMSO, a good solvent (Fig. S18). In contrast, the particles synthesized using LED₃₆₅ dissolved completely in DMSO (Fig. S19). Thus, interfacial photocycloaddition polymerization proceeds at wavelengths that are absorbed by photoreactive monomers.

Dye and fragrance polymer capsules

The photocycloaddition reaction occurs with a 100% atom economy and does not involve any leaving groups. Thus, the

polymer shells of the hollow particles fabricated by interfacial photocycloaddition polymerization were assumed to comprise a dense structure without pores that would allow various molecules to leak out. First, the encapsulation stability of the hollow polymer particles was investigated using a fluorescent dye model compound. The hollow polymer particles were incubated in DMSO to dissolve the fluorescent dye (sulforhodamine B). In DMSO, the crosslinked polymer shell swelled and the fluorescent dye diffused into the interior of the polymer particles. Subsequently, fluorescent-dye-incorporated polymer capsules were obtained by polymer shell shrinkage *via* solvent exchange with an aqueous poly(vinyl alcohol) solution (Fig. 3a). In the CLSM image of the sulforhodamine B-encapsulated P(dCP-tCG) particles, fluorescence derived from the dye was observed inside the P(dCP-tCG) particles, with negligible fluorescence in the polymer shell, confirming the encapsulation of sulforhodamine B (an anionic molecule) (Fig. 3b and c). Subsequently, for the encapsulation stability analysis, the dye-encapsulated P(dCP-tCG) capsules were incubated in pure water; negligible dye leakage was observed in the supernatant after 10 days (Fig. S20). Furthermore, fluorescence derived from sulforhodamine B was clearly observed in the P(dCP-tCG) capsules even after three months in PVA aqueous solution (Fig. S21 and S22). These results confirmed the high encapsulation stability of the P(dCP-tCG) particles with low-molecular-weight dyes. In an additional experiment conducted during the course of this study, fluorescence was still detectable inside the capsules even after 13 months, further demonstrating the long-term stability of the capsule shell (Fig. S23).

As a practical application of their highly stable encapsulation ability, the hollow P(dCP-tCG) particles were used to prepare fragrance capsules. Limonene, a typical monocyclic monoterpene found in citrus fruits, emits a natural fragrance. To investigate the encapsulation stability of the hollow P(dCP-tCG) particles toward limonene, limonene-encapsulated P(dCP-tCG) particles were synthesized by the solvent-exchange procedure shown in Fig. 3a. Polymer capsules were placed statically in closed vials for one day with stirring (for physical destruction of capsules) or without stirring with a stirring bar, followed by gas phase analysis using gas chromatography. SEM observations after physical destruction of the P(dCP-tCG) capsules clearly showed the presence of fragmented particles (Fig. S24). The chromatogram for the unstirred polymer capsules does not contain the limonene peak (Fig. 3d and e), confirming stable limonene encapsulation by P(dCP-tCG). Notably, a limonene peak was detected after the physical destruction of the polymer capsule by stirring (Fig. 3e). Furthermore, fragrance capsules containing higher limonene concentrations (~90 vol%) could be prepared by increasing the limonene concentration of the solution for the encapsulation process (Fig. S25). Thus, fragrance capsules were successfully prepared using hollow P(dCP-tCG) particles synthesized *via* interfacial photocycloaddition polymerization.

Degradability of polymer capsules

The $[2\pi + 2\pi]$ photodimerization between cinnamate groups is an elemental reaction in interfacial photocycloaddition polymerization, which is reversible.⁴⁰ The retro-photodimerization reaction

requires irradiation with short-wavelength light because the absorption wavelength of the cinnamate dimer is shifted to shorter wavelengths compared to that of the cinnamate monomer. Previously, the reversibility of photodimerization was used for reversible polymer ligation,⁴¹ topological control of polymers,⁴² reversible patterning,⁴³ drug delivery,⁴⁴ and synthesis of hydrogels capable of sol-gel transitions.⁴⁵ Thus, the hollow P(dCP-tCG) particles synthesized in this study are intrinsically photodegradable. In this study, the photodegradation of crosslinked hollow P(dCP-tCG) particles was investigated under photoirradiation at 254 nm in DMSO (Fig. 4a). In this case, irradiation with short-wavelength light induces retro-photocycloaddition reactions that reduce the crosslink density of the hollow particle shell, ultimately leading to degradation into the monomeric form. Here, the molecules generated by photolysis (depolymerization) from the hollow particles are dissolved and diluted in DMSO, so that the photolysis (depolymerization) is considered to proceed predominantly. With increasing photoirradiation time, the transmittance of the dispersed particles at 600 nm decreased (Fig. 4c and d), and the absorbance of the free cinnamate groups at 280 nm gradually increased, indicating that the retro-photocycloaddition reaction occurred and the dimerized cinnamate groups were converted into cinnamate monomers (Fig. 4b). Furthermore, the regenerated photoreactive monomer was successfully detected after photolysis of the P(dCP-tCG) hollow particles by MALDI-TOF-MS (Fig. S26). These results confirmed the photodegradation of hollow P(dCP-tCG) particles by short-wavelength light. The P(dCP-tCG) particles contain an ester linkage in the polymer main chain; thus, the hydrolytic degradability of the hollow P(dCP-tCG) particles was investigated (Fig. 4e). The hollow P(dCP-tCG) particles were incubated in an aqueous solution of 10 mM NaOH water/DMSO mixture, and the transmittance of the particle dispersion was investigated. The ester linkage was hydrolyzed during the degradation test, and the polymer was degraded into glycerin, cinnamate anions, cinnamate anion dimers, and oligomers. Owing to hydrolysis, the transmittance gradually increased with prolonged incubation, suggesting that cleavage of the ester bonds within the crosslinked polymer forming the shell of the hollow particles resulted in a reduction of the crosslink density and led to fragmentation (Fig. 4f and g). Furthermore, ¹H-NMR analysis of the hydrolyzed molecules indicated that the crosslinked polymer shells synthesized by interfacial photocycloaddition polymerization contained ~18.5% unreacted cinnamate groups (Fig. S27).

Regulation of the reactive wavelength for interfacial photocycloaddition polymerization

The regulation of the reaction wavelength for interfacial photocycloaddition polymerization was investigated by introducing substituents on the cinnamate groups. To increase the reaction wavelength, nitro, methoxy, and dimethylamino groups were introduced at the *para*-positions of the cinnamate groups. Bifunctional photoreactive monomers were synthesized by the coupling reaction between 1,5-pentanediol and para-substituted cinnamic acids (*i.e.*, *p*-nitro cinnamic acid: dNO₂CP, *p*-methoxy cinnamic acid: dOMeCP, and *p*-dimethylamino cinnamic acid: dNMe₂CP) (Fig. 5a and S28–S33). Trifunctional photoreactive

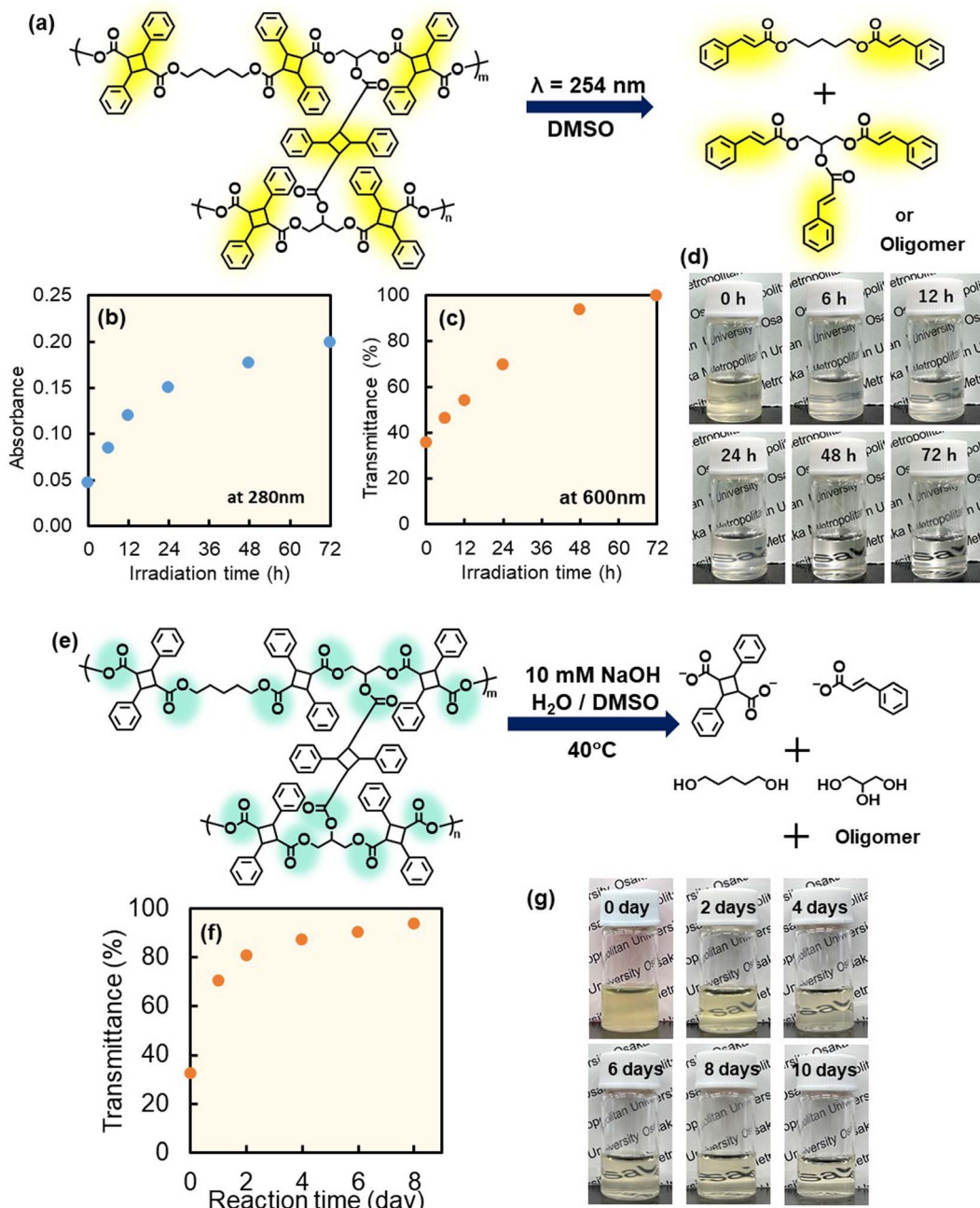


Fig. 4 Schematic of the retro-photocycloaddition polymerization of hollow P(dCP-tCG) particles synthesized by interfacial photocycloaddition polymerization (a). Absorbance of the free cinnamate groups at 280 nm (b) and transmittance of the dispersed hollow polymer particles at 600 nm (c) after photoirradiation at 254 nm for various durations. Dispersion of P(dCP-tCG) hollow particles before and after retro-photocycloaddition polymerization when subjected to photoirradiation at 254 nm for various durations (d). Schematic of the hydrolysis of ester linkages in hollow P(dCP-tCG) particles synthesized by interfacial photocycloaddition polymerization (e). Transmittance of the dispersion containing hollow P(dCP-tCG) particles at 600 nm after hydrolysis for different reaction times (f). Dispersion of hollow P(dCP-tCG) particles before and after hydrolysis for various reaction times (g).

monomers were also synthesized by coupling glycerin with para-substituted cinnamic acids (*i.e.*, *p*-nitro cinnamic acid: tNO₂CG, *p*-methoxy cinnamic acid: tOMeCG, and *p*-dimethylamino cinnamic acid: tNMe₂CG) (Fig. 5a and S34–S39). The maximum absorption wavelengths of dNO₂CP, dOMeCP, and dNMe₂CP, as indicated by UV-vis spectroscopy, were 310, 315, and 370 nm, respectively (Fig. 5b–d). The maximum absorption wavelengths of tNO₂CG, tOMeCG, and tNMe₂CG were ~310, 315, and 370 nm,

respectively (Fig. S40–S42). The monomer particles were synthesized using a homogenizer and bi- and trifunctional monomers with the same substituents, and interfacial photocycloaddition polymerization was conducted using LED light of different wavelengths. Hollow polymer particles comprising dNO₂CP/tNO₂CG and dOMeCP/tOMeCG were synthesized by interfacial photocycloaddition polymerization of the relevant monomer particles using a long-wavelength LED ($\lambda = 365$ nm: LED₃₆₅) (Fig. S43).

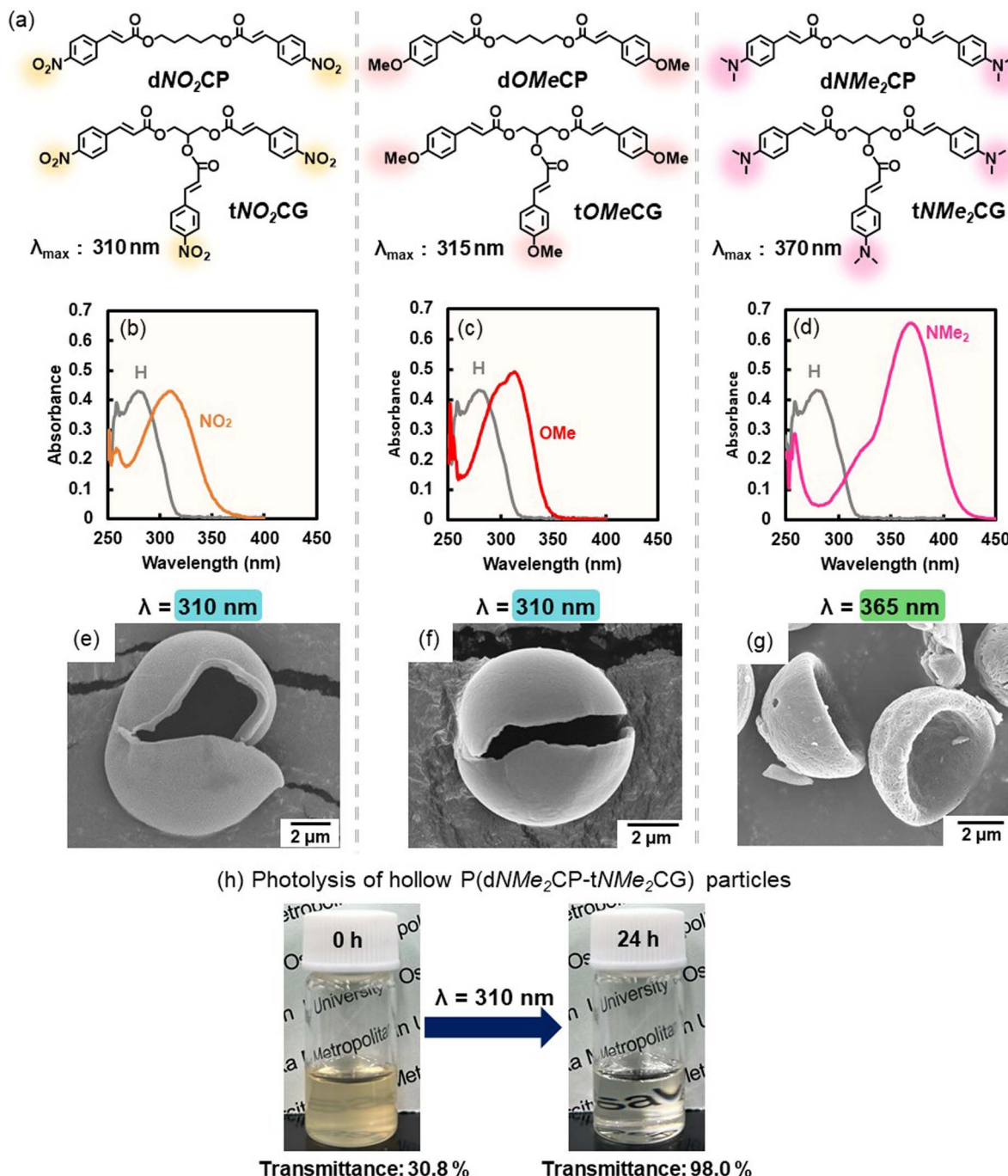


Fig. 5 Chemical structures of **dNO₂CP**, **tNO₂CG**, **dOMeCP**, **tOMeCG**, **dNMe₂CP**, and **tNMe₂CG** (a), and UV-vis spectra of **dNO₂CP** (b), **dOMeCP** (c), and **dNMe₂CP** (d). SEM images of hollow polymer particles fabricated by interfacial photocycloaddition polymerization of **dNO₂CP-tNO₂CG** (e), **dOMeCP-tOMeCG** (f), and **dNMe₂CP-tNMe₂CG** (g). Dispersion of hollow **P(dNMe₂CP-tNMe₂CG)** particles before and after retro-photocycloaddition polymerization for 24 h upon photoirradiation at 310 nm (h).

Furthermore, hollow **P(dNMe₂CP-tNMe₂CG)** particles could be synthesized using 365-nm, 410-nm, and 465-nm LED light (LED_{365} , LED_{410} , and LED_{465} , respectively; Fig. S44 and S45). Thus, the reaction wavelength for interfacial photocycloaddition polymerization can be regulated by introducing substituents into the photoreactive monomers. Notably, the **P(dNO₂CP-tNO₂CG)**,

P(dOMeCP-tOMeCG), and **P(dNMe₂CP-tNMe₂CG)** particles can stably encapsulate sulforhodamine B (Fig. S46–S48).

To investigate the photodegradation of the polymer particles with longer-wavelength light, hollow **P(dNMe₂CP-tNMe₂CG)** particles were photoirradiated with LED_{310} . With increasing photoirradiation time, the transmittance from the dispersion containing hollow polymer particles gradually increased (Fig. 5h).



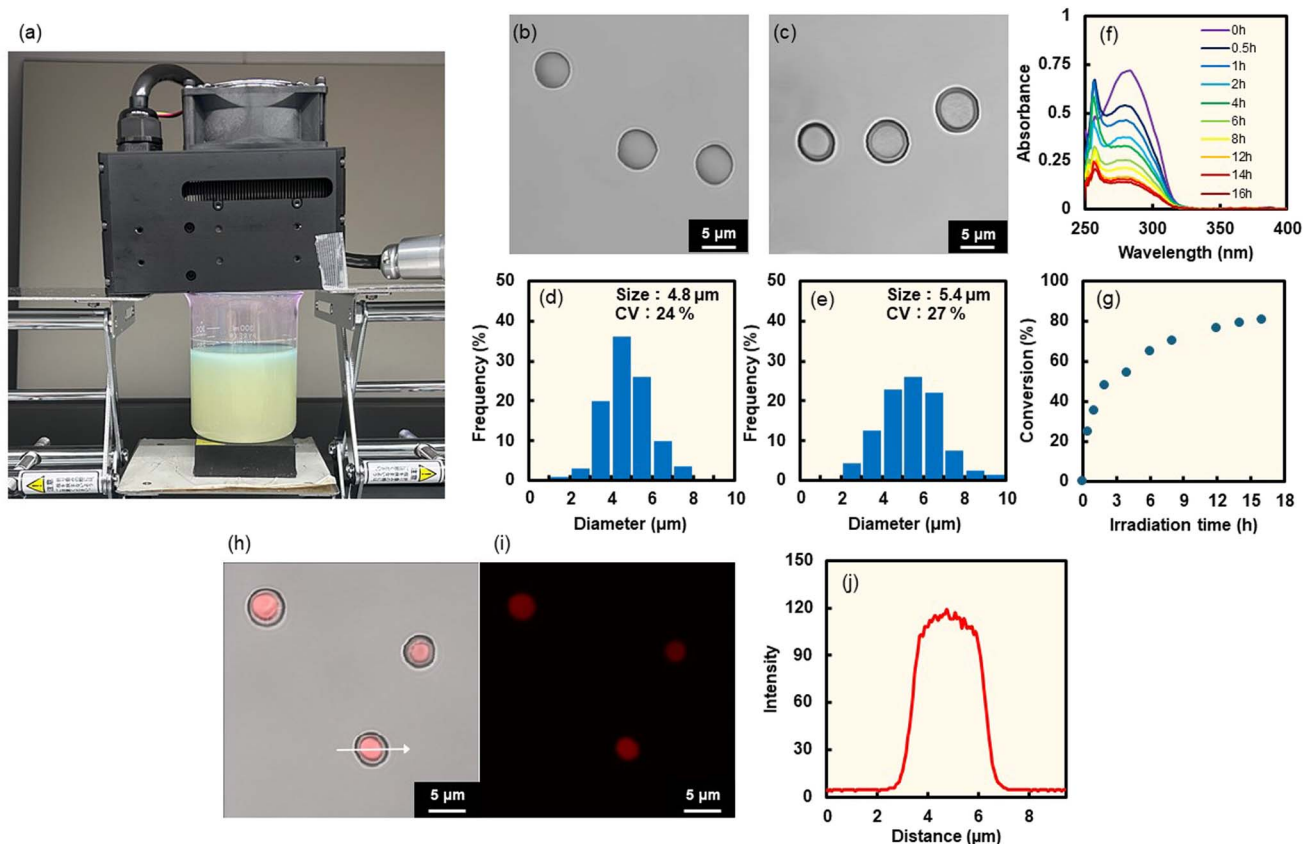


Fig. 6 Photograph of the scale-up synthesis of hollow P(dCP-tCG) particles by interfacial photocycloaddition polymerization (a). Optical microscopy images (b, c) and particle size distributions (d and e) of the monomer particles used as starting materials (b, d) and hollow particles synthesized through interfacial photocycloaddition polymerization (c and e). UV-vis spectra (f) and conversion (%) (g) derived from non-reacted cinnamates after interfacial photocycloaddition polymerization for various photoirradiation times in the scaled-up synthesis. Bright-field (h), CLSM (i) images, and line profile of the fluorescence intensity of the CLSM image (j) of sulforhodamine B-encapsulated P(dCP-tCG) particles synthesized on a large scale.

Thus, the photodegradation wavelength of the photopolymerized hollow particles could also be regulated by introducing substituents into the photoreactive groups in the system.

Interfacial photocycloaddition polymerization with high-power LED light

Finally, experiments were conducted for the synthesis of hollow polymer particles by interfacial photocycloaddition polymerization with high-power LED light, thereby demonstrating the potential for a 100-fold increase in scale. For the synthesis, high-power LED₂₆₅ light (14 mW cm⁻²) with a wide irradiation area (900 mm²) was used (Fig. 6a). In addition, monomer particles comprising dCP and tCG dispersed in aqueous PVA media with a 100 times larger scale (total monomer weight: 200 mg; dispersion volume: 300 mL) were synthesized using a homogenizer (Fig. 6b and d). Hollow P(dCP-tCG) particles were obtained after 16 h of photocycloaddition polymerization and subsequent washing (Fig. 6c and e-g). Furthermore, the hollow P(dCP-tCG) particles stably encapsulated sulforhodamine B (Fig. 6h-j). Thus, the interfacial photocycloaddition polymerization successfully proceeded with high-power LED light, yielding the hollow P(dCP-tCG) particles with a 100-fold increase in scale.

Conclusions

In this study, interfacial photocycloaddition polymerization was developed as a novel approach for fabricating photolysis- and hydrolysis-induced degradable polymer particles possessing structural functions, using di- and tri-functionalized photoreactive monomers derived from natural compounds. The hollow particles stably encapsulated low-molecular-weight compounds. The polymer capsules showed negligible leakage of encapsulated sulforhodamine B, even after several months of storage, and were efficiently degraded upon exposure to short-wavelength LED light or hydrolysis under alkaline conditions. In the long term, we believe that the particulate material will degrade into the natural molecules constituting the photoresponsive monomers due to the photolytic and hydrolytic degradability. Experimental evaluation of the environmental degradability and monomer recyclability will be addressed in future work. Furthermore, the photoreactive wavelength could be regulated using para-substituted photoreactive monomers, that is, nitro- and methoxy-substituted monomers could be polymerized in the range of LED₃₁₀-LED₃₆₅ and dimethylamino-substituted monomers could be polymerized in the range of LED₃₆₅-LED₄₆₅. Importantly, the photolysis wavelength was shifted to a longer wavelength (310 nm) when



dimethylamino-substituted monomers were used for polymer capsule fabrication. Finally, the scaled-up synthesis of the polymer capsules *via* interfacial photocycloaddition polymerization was possible using a high-power LED lamp. We will demonstrate the interfacial photocycloaddition polymerization using flow reactors for effective scale-up synthesis in the near future.

Author contributions

Y. Kitayama conceived and supervised the project and wrote the manuscript. M. Yamashita carried out the experiments and data analysis. M. Yamashita and A. Harada reviewed and provided feedback on the manuscript.

Conflicts of interest

The authors declare no competing financial interest.

Data availability

The data supporting this article have been included as part of the supplementary information (SI). Supplementary information: materials, apparatus, UV-vis spectra, NMR spectra for photoreactive monomers, synthesis of fluorescein-labeled photoreactive monomers, photoreactive monomers possessing different substituents, and experimental results of interfacial photocycloaddition polymerization with different wavelength. See DOI: <https://doi.org/10.1039/d5sc07979a>.

Acknowledgements

This study was supported by JST PRESTO Grant Number JPMJPR24M3, Japan (for YK), and JSPS KAKENHI (grant numbers 21H02004, 23K21137, and 24K01559 for YK). This study was partially supported by the Leading Initiative for Excellent Young Researchers (MEXT, Japan) (for YK). We deeply thank Ms. Yukiko Miyaji (Sakamoto Yakuhin Kogyo Co., Ltd) for supplying glycerin.

References

- 1 J. Gaitzsch, X. Huang and B. Voit, Engineering Functional Polymer Capsules toward Smart Nanoreactors, *Chem. Rev.*, 2016, **116**(3), 1053–1093.
- 2 S. F. M. Van Dongen, H. P. M. De Hoog, R. J. R. W. Peters, M. Nallani, R. J. M. Nolte and J. C. M. Van Hest, Biohybrid polymer capsules, *Chem. Rev.*, 2009, **109**(11), 6212–6274.
- 3 J. Cui, M. P. Van Koeverden, M. Müllner, K. Kempe and F. Caruso, Emerging methods for the fabrication of polymer capsules, *Adv. Colloid Interface Sci.*, 2014, **207**(1), 14–31.
- 4 A. Özsevinç and C. Alkan, Ethylene glycol based polyurethane shell microcapsules for textile applications releasing medicinal lavender and responding to mechanical stimuli, *Colloids Surf., A*, 2022, 652.
- 5 B. Peña, C. Panisello, G. Aresté, R. Garcia-Valls and T. Gumí, Preparation and characterization of polysulfone microcapsules for perfume release, *Chem.-Eng. J.*, 2012, **179**, 394–403.
- 6 X. Qiu, Y. Li, Y. Qian, J. Wang and S. Zhu, Long-Acting and Safe Sunscreens with Ultrahigh Sun Protection Factor *via* Natural Lignin Encapsulation and Synergy, *ACS Appl. Bio Mater.*, 2018, **1**(5), 1276–1285.
- 7 T. O. Machado, J. Grabow, C. Sayer, P. H. H. de Araújo, M. L. Ehrenhard and F. R. Wurm, Biopolymer-based nanocarriers for sustained release of agrochemicals: a review on materials and social science perspectives for a sustainable future of agri- and horticulture, *Adv. Colloid Interface Sci.*, 2022, **303**, 102645.
- 8 S. H. Im, U. Y. Jeong and Y. N. Xia, Polymer hollow particles with controllable holes in their surfaces, *Nat. Mat.*, 2005, **4**(9), 671–675.
- 9 N. Han, M. G. Kim, S. W. Kim, M. K. Shin, S. J. Kim, M. S. Kim, S. R. Lee, J. B. Lee, S. B. Pyun, J. A. La, J. E. Song and E. C. Cho, Enhanced Near-Infrared Shielding and Light Scattering Using Surface-Roughened Hybrid Hollow Microparticles Synthesized with Polymer and $\text{TiO}_2@\text{Al(OH)}_3$ for Cosmetic Applications, *Part. Part. Syst. Charact.*, 2018, **35**(6), 1800057.
- 10 W. Wichaita, D. Polpanich and P. Tangboriboonrat, Review on Synthesis of Colloidal Hollow Particles and Their Applications, *Ind. Eng. Chem. Res.*, 2019, **58**(46), 20880–20901.
- 11 A. Belostozky, S. Bretler, M. Kolitz-Domb, I. Grinberg and S. Margel, Solidification of oil liquids by encapsulation within porous hollow silica microspheres of narrow size distribution for pharmaceutical and cosmetic applications, *Mater. Sci. Eng., C*, 2019, **97**, 760–767.
- 12 F. Wang, C. S. Wong, D. Chen, X. Lu, F. Wang and E. Y. Zeng, Interaction of toxic chemicals with microplastics: a critical review, *Water Res.*, 2018, **139**, 208–219.
- 13 M. Cole, P. Lindeque, E. Fileman, C. Halsband, R. Goodhead, J. Moger and T. S. Galloway, Microplastic ingestion by zooplankton, *Environ. Sci. Technol.*, 2013, **47**(12), 6646–6655.
- 14 A. ter Halle, L. Ladirat, M. Martignac, A. F. Mingotaud, O. Boyron and E. Perez, To what extent are microplastics from the open ocean weathered?, *Environ. Pollut.*, 2017, **227**, 167–174.
- 15 B. Biswas, A. Joseph, V. P. Ranjan and S. Goel, Adsorption of Emerging Contaminants on Microplastics in the Environment: a Systematic Review, *ACS ES&T Water*, 2024, **4**(12), 5207–5224.
- 16 A. L. Lusher, M. McHugh and R. C. Thompson, Occurrence of microplastics in the gastrointestinal tract of pelagic and demersal fish from the English Channel, *Mar. Pollut. Bull.*, 2013, **67**(1–2), 94–99.
- 17 L. G. A. Barboza, A. Dick Vethaak, B. R. B. O. Lavorante, A. K. Lundebye and L. Guilhermino, Marine microplastic debris: an emerging issue for food security, food safety and human health, *Mar. Pollut. Bull.*, 2018, **133**, 336–348.
- 18 M. Smith, D. C. Love, C. M. Rochman and R. A. Neff, Microplastics in Seafood and the Implications for Human Health, *Curr. Environ. Health Rep.*, 2018, **5**(3), 375–386.



19 J. J. Richardson, J. W. Cui, M. Bjornmalm, J. A. Braunger, H. Ejima and F. Caruso, Innovation in Layer-by-Layer Assembly, *Chem. Rev.*, 2016, **116**(23), 14828–14867.

20 A. P. R. Johnston, C. Cortez, A. S. Angelatos and F. Caruso, Layer-by-layer engineered capsules and their applications, *Curr. Opin. Colloid Interface Sci.*, 2006, **11**(4), 203–209.

21 X. L. Xu and S. A. Asher, Synthesis and utilization of monodisperse hollow polymeric particles in photonic crystals, *J. Am. Chem. Soc.*, 2004, **126**(25), 7940–7945.

22 K. Ohno, T. Morinaga, K. Koh, Y. Tsujii and T. Fukuda, Synthesis of monodisperse silica particles coated with well-defined, high-density polymer brushes by surface-initiated atom transfer radical polymerization, *Macromolecules*, 2005, **38**(6), 2137–2142.

23 H. Minami, H. Kanamori, Y. Hata and M. Okubo, Preparation of microcapsules containing a curing agent for epoxy resin by polyaddition reaction with the self-assembly of phase-separated polymer method in an aqueous dispersed system, *Langmuir*, 2008, **24**(17), 9254–9259.

24 C. Scott, D. Wu, C. C. Ho and C. C. Co, Liquid-core capsules via interfacial polymerization: a free-radical analogy of the nylon rope trick, *J. Am. Chem. Soc.*, 2005, **127**(12), 4160–4161.

25 F. J. Lu, Y. W. Luo and B. G. Li, A facile route to synthesize highly uniform nanocapsules: use of amphiphilic poly(acrylic acid)-block-polystyrene RAFT agents to interfacially confine miniemulsion polymerization, *Macromol. Rapid Commun. Macromolecules*, 2007, **28**(7), 868–874.

26 F. Ishizuka, M. H. Stenzel and P. B. Zetterlund, Microcapsule synthesis via RAFT photopolymerization in vegetable Oil as a green solvent, *J. Polym. Sci., Part A: Polym. Chem.*, 2018, **56**(8), 831–839.

27 Y. Wang, P. Wei, Q. Zhou, C. Cipriani, M. Qi, S. Sukhishvili and E. Pentzer, Temperature-Dependent Capsule Shell Bonding and Destruction Based on Hindered Poly(urethane) Chemistry, *Chem. Mater.*, 2022, **34**(13), 5821–5831.

28 L. Torini, J. F. Argillier and N. Zydowicz, Interfacial polycondensation encapsulation in miniemulsion, *Macromolecules*, 2005, **38**(8), 3225–3236.

29 Y. Kitayama, K. Yoshikawa and T. Takeuchi, Efficient pathway for preparing hollow particles: site-specific crosslinking of spherical polymer particles with photoresponsive groups that play a dual role in shell crosslinking and core shielding, *Langmuir*, 2016, **32**(36), 9245–9253.

30 Y. Kitayama and A. Harada, PH-Responsive Capsule Polymer Particles Prepared by Interfacial Photo-Cross-Linking: Effect of the Alkyl Chain Length of the pH-Responsive Monomer, *ACS Appl. Mater. Interfaces*, 2021, **13**(29), 34973–34983.

31 Y. Kitayama and A. Harada, Interfacial Photo-Cross-Linking: Simple but Powerful Approach for Fabricating Capsule Polymer Particles with Tunable pH-Responsive Controlled Release Capability, *ACS Appl. Mater. Interfaces*, 2021, **13**(8), 10359–10375.

32 Y. Kitayama and T. Takeuchi, Fabrication of Redox-Responsive Degradable Capsule Particles by a Shell-Selective Photoinduced Cross-Linking Approach from Spherical Polymer Particles, *Chem. - Eur. J.*, 2017, **23**(52), 12870–12875.

33 Y. Kitayama and T. Takeuchi, Photodegradable Polymer Capsules Fabricated via Interfacial Photocross-linking of Spherical Polymer Particles, *ACS Appl. Polym. Mater.*, 2020, **2**(9), 3813–3820.

34 J. Wang, C. Li, Y. Zou and Y. Yan, Bacterial synthesis of C3–C5 diols via extending amino acid catabolism, *Proc. Natl. Acad. Sci. U. S. A.*, 2020, **117**(32), 19159–19167.

35 X. Cen, Y. Liu, B. Chen, D. Liu and Z. Chen, Metabolic Engineering of *Escherichia coli* for *de Novo* Production of 1,5-Pentanediol from Glucose, *ACS Synth. Biol.*, 2021, **10**(1), 192–203.

36 Y. Tokitomo, M. Steinhaus, A. Buettner and P. Schieberle, Odor-active constituents in fresh pineapple (*Ananas comosus* [L.] Merr.) by quantitative and sensory evaluation, *Biosci., Biotechnol., Biochem.*, 2005, **69**(7), 1323–1330.

37 P. Schieberle and T. Hofmann, Evaluation of the Character Impact Odorants in Fresh Strawberry Juice by Quantitative Measurements and Sensory Studies on Model Mixtures, *J. Agric. Food Chem.*, 1997, **45**(1), 227–232.

38 T. W. Pearson, H. J. Dawson and H. B. Lackey, Natural Occurring Levels of Dimethyl Sulfoxide in Selected Fruits, Vegetables, Grains, and Beverages, *J. Agric. Food Chem.*, 1981, **29**(5), 1089–1091.

39 M. O. Andreea, Ocean-atmosphere interactions in the global biogeochemical sulfur cycle, *Mar. Chem.*, 1990, **30**(C), 1–29.

40 H. Frisch, K. Mundsinger, B. L. J. Poad, S. J. Blanksby and C. Barner-Kowollik, Wavelength-gated photoreversible polymerization and topology control, *Chem. Sci.*, 2020, **11**(10), 2834–2842.

41 D. E. Marschner, H. Frisch, J. T. Offenloch, B. T. Tuten, C. R. Becer, A. Walther, A. S. Goldmann, P. Tzvetkova and C. Barner-Kowollik, Visible Light [2 + 2] Cycloadditions for Reversible Polymer Ligation, *Macromolecules*, 2018, **51**(10), 3802–3807.

42 T. Yamamoto, S. Yagyu and Y. Tezuka, Light- and Heat-Triggered Reversible Linear-Cyclic Topological Conversion of Telechelic Polymers with Anthryl End Groups, *J. Am. Chem. Soc.*, 2016, **138**(11), 3904–3911.

43 Q. Yan, L. Mao, B. Feng, L. Zhang, Y. Wu and W. Huang, Reversible Patterning Cross-Linked, Humidity-Responsive Polymer Films with Programmatically and Accurately Controlled Deformation, *ACS Appl. Mater. Interfaces*, 2021, **13**(6), 7608–7616.

44 L. A. Wells, S. Furukawa and H. Sheardown, Photoresponsive PEG-anthracene grafted hyaluronan as a controlled-delivery biomaterial, *Biomacromolecules*, 2011, **12**(4), 923–932.

45 C. P. Kabb, C. S. O'Bryan, C. C. Deng, T. E. Angelini and B. S. Sumerlin, Photoreversible Covalent Hydrogels for Soft-Matter Additive Manufacturing, *ACS Appl. Mater. Interfaces*, 2018, **10**(19), 16793–16801.

